Biosensors and Bioelectronics 31 (2012) 439–444

Contents lists available at SciVerse ScienceDirect

Biosensors and Bioelectronics

journal homepage: www.elsevier.com/locate/bios

Sensing HIV related protein using epitope imprinted hydrophilic polymer coated quartz crystal microbalance

Chun-Hua Lu[a], Yan Zhang[a], Shui-Fen Tang[a], Zhi-Bin Fang[a], Huang-Hao Yang[a,*], Xi Chen[b,**], Guo-Nan Chen[a]

[a] The Key Lab of Analysis and Detection Technology for Food Safety of the MOE, Fujian Provincial Key Laboratory of Analysis and Detection Technology for Food Safety, College of Chemistry and Chemical Engineering, Fuzhou University, Fuzhou 350002, PR China
[b] State Key Laboratory of Marine Environmental Science, Xiamen University, Xiamen 361005, PR China

ARTICLE INFO

Article history:
Received 19 October 2011
Accepted 4 November 2011
Available online 15 November 2011

Keywords:
Dopamine
Epitope imprinting
HIV-1
Molecularly imprinted polymers
Quartz crystal microbalance

ABSTRACT

We have developed a biomimetic sensor for the detection of human immunodeficiency virus type 1 (HIV-1) related protein (glycoprotein 41, gp41) based on epitope imprinting technique. gp41 is the transmembrane protein of HIV-1 and plays an important role in membrane fusion between viruses and infected cells. It is an important index for determining the extent of HIV-1 disease progression and the efficacy of therapeutic intervention. In this work, dopamine was used as the functional monomer and polymerized on the surface of quartz crystal microbalance (QCM) chip in the presence of template, a synthetic peptide with 35 amino acid residues, analogous to residues 579–613 of the gp41. This process resulted in grafting a hydrophilic molecularly imprinted polymer (MIP) film on the QCM chip. QCM measurement showed that the resulting MIP film not only had a great affinity towards the template peptide, but also could bind the corresponding gp41 protein specifically. The dissociation constant (K_d) of MIP for the template peptide was calculated to be 3.17 nM through Scatchard analysis, which was similar to those of monoclonal antibodies. Direct detection of the gp41 was achieved quantitatively using the resulting MIP-based biomimetic sensor. The detection limit of gp41 was 2 ng/mL, which was comparable to the reported ELISA method. In addition, the practical analytical performance of the sensor was examined by evaluating the detection of gp41 in human urine samples with satisfactory results.

1. Introduction

The concept of molecularly imprinted polymers (MIPs) has a long history dating back to the early 1930s (Polyakov, 1931). MIPs are artificial made receptors with the ability to recognize and to specially bind the target molecule (Wulff and Sarhan, 1972; Wulff, 1995; Vlatakis et al., 1993). The synthesis of MIPs involves the formation of a complex of a target molecule (template) with one or more functional monomers though either covalent or noncovalent bonds followed by a polymerization reaction with cross-linking agent. Upon removal of the template, the binding sits are produced that are complementary to the template in shape, size, and the position of the functional groups. The stability, ease of preparation, and low cost of MIPs have led to their assessment as substitutes for antibodies or enzymes in sensors, catalysis, and separations (Haupt, 2003; Alexander et al., 2006; Ye and Mosbach, 2008; Ge and Turner, 2009). Although creating a MIP against small molecules (Wang et al., 2006; Gao et al., 2007; Riskin et al., 2008, 2009; Tan et al., 2009; Bui et al., 2010; Stringer et al., 2010; Pernites et al., 2011; Li et al., 2011) or peptides (Hoshino et al., 2008; Zeng et al., 2010) is straightforward now, imprinting of large structures, such as proteins and other biomacromolecules, is still a challenge (Shi et al., 1999; Bossi et al., 2001, 2007; Ge and Turner, 2008; Cutivet et al., 2009; He et al., 2010; Cai et al., 2010; Zhang et al., 2011). The major problem associated with the imprinting of proteins lies in their restricted mobility within highly cross-linked polymer networks and the poor efficiency in rebinding. Meanwhile, the molecular size, conformational flexibility and sensitivity to denaturation of proteins would also make them difficult for imprinting. Consequently, some approaches, such as surface imprinting (Li et al., 2006; Tatemichi et al., 2007; Nematollahzadeh et al., 2011) and epitope imprinting (Rachkov and Minour, 2000; Tai et al., 2005, 2010; Nishino et al., 2006), have been developed to overcome these problems.

Epitope imprinting is first demonstrated by Minoura and coworkers for peptide recognition (Rachkov and Minour, 2000). In this process, a fragment exposed on the epitope of the target

* Corresponding author. Tel.: +86 591 22866135; fax: +86 591 22866135.
** Corresponding author.
E-mail addresses: hhyang@fio.org.cn (H.-H. Yang), xichen@xmu.edu.cn (X. Chen).

0956-5663/$ – see front matter © 2011 Elsevier B.V. All rights reserved.
doi:10.1016/j.bios.2011.11.008

macromolecular is used as template, the resultant MIP recognize not only the template but also the whole macromolecule. For example, in 2006, Shea and coworkers use the epitope-peptides of cytochrome C and bovine serum albumin as templates for creating macromolecular receptors for proteins (Nishino et al., 2006). Recently, Tai and coworkers developed a MIP-coated quartz crystal microbalance sensor for the dengue virus NS1 protein using epitope-mediated imprinting (Tai et al., 2010). Compared with traditional protein imprinting approaches, epitope imprinting has several advantages (Ge and Turner, 2008). Firstly, more specific and stronger interactions with a fragment or small part of the macromolecule can lower the non-specific binding and improve the affinity. Secondly, the polymer can not only recognize the template but also the entire protein and the operation procedures are easier. Thirdly, the short peptides as the epitopes for imprinting are low cost. However, little work of epitope imprinting has been conducted for detection of proteins in real human fluid samples.

HIV-1 glycoprotein 41 (HIV-1 gp41) is a protein that sits in the virus coat of human immunodeficiency virus type 1 (HIV-1), which is the causative agent of the acquired immunodeficiency syndrome (AIDS) (Contreras et al., 2001). It locates in the phospholipids bilayer and plays an important role in membrane fusion between viruses and target cells upon gp120 binding of CD4. After the viral attaching to cells, gp41 is thought to undergo a conformational change to mediate the fusion of the viral and target cell membranes (Dwyer et al., 2003; Burton et al., 2004; Buzón and Cladera, 2006). gp41 is an important protein that is not only relevant in fusion, but its activation process may provide novel strategies for vaccine and antiviral drug development (Chan et al., 1998). Therefore, developing a convenient, sensitive method for determination of gp41 is of great meaning in early clinical diagnosis and pathogenetic condition monitoring.

In this work, a MIP-coated quartz crystal microbalance (QCM) biomimetic sensor for the gp41 protein was fabricated by epitope-imprinting techniques. Dopamine was used as functional monomer and a synthetic peptide with 35 amino acid residues, analogous to residues 579–613 of the HIV-1 gp41 was used as the template. gp41 fragment 579–613 is a major immunodominant region that can be recognized by antibodies from approximately 98% of AIDS patients. Commonly known as a neurotransmitter, dopamine is also a small-molecule mimic of the adhesive proteins. Recently, Messersmith reported a simple but versatile surface modification approach in which self-polymerization of dopamine at weak alkaline pH produced an adherent polydopamine coating on a wide variety of materials including noble metals, oxides, semiconductors, and ceramics (Lee et al., 2007). The polydopamine films were found to be a versatile platform for further modification, leading to tailoring of the films for diverse functional uses (Lee et al., 2007). The detailed understanding of the polymerization mechanism of polydopamine was unknown so far. The prevalent view was that in alkaline conditions catechol was easily oxidized to quinone form, and the cross-linking was attributed to the reverse dismutation reaction between catechol and quinone form of dopamine molecule (Burzio and Waite, 2000; van der Leeden, 2005). Recently, polydopamine has been used successfully for molecular imprinting due to the high stability, hydrophilicity and biocompatibility (Ouyang et al., 2007, 2008; Zhou et al., 2010). However, there is no report about the application of polydopamine in epitope-imprinting. In this work, we demonstrated that the epitope-imprinting polydopamine film can not only recognize the template but also recognize the corresponding protein. Furthermore, this new method offers several advantages such as easy preparation, high stability and sensitivity, which would make this approach more practical in detection and separation of bio-samples.

2. Materials and methods

2.1. Materials

The synthetic peptide of gp41 fragment 579–613 (RILA VERY LKDQ QLLG IWGC SGKL ICTT AVPW NAS), peptide with two mutated (underlined) residues (2M-peptide) (RILA VERY LKDQ Q**AA**G IWGC SGKL ICTT AVPW NAS), peptide with eleven mutated residues (11M-peptide) (RILA VE**AA** L**AAA** QLLG IWGC **A**G**A**L IC**AA** AV**AA** NAS), and the control peptide with thirty amino acid residues (FHLL REML EMAK AEQE AEQA ALNR LLLE EA) were purchased from the Beijing Biosynthesis Biotechnology Co., Ltd, China. Dopamine hydrochloride was from Sigma–Aldrich. Ammonium persulfate was from Alfa Aesar. Bovine serum albumin (BSA), Tris(hydroxymethyl)aminomethane hydrochloride (Tris–HCl), and other chemicals of analytical reagent grade were obtained from Sinopharm Chemical Reagent Co., Ltd. All water used was obtained from a Millipore Milli-Q purification system.

2.2. Instrument

The QCM (KSV model QCM-Z500) was obtained from KSV Instruments Ltd (KSV, Finland). AT-cut planar silicon oxide-coated QCM chips (14 mm diameter) with a nominal resonance frequency of 5 MHz (4.95 MHz ± 50 kHz) were supplied by Q-sense (Q-sense, Swedish). Atomic force microscopic (AFM) images were taken out using a Nanoscope IIIa multimode atomic force microscope (Veeco Instruments, USA). The Fourier-transform infrared spectroscopy (FT-IR) spectrum was recorded on a Nicolet 6700 spectrometer (Thermo Electron Corporation, USA). The chemical composition was investigated by X-ray photoelectron spectrometer (XPS) model ESCALAB 250 (Thermo Electron Corporation, USA).

2.3. Preparation of molecularly imprinted polymer (MIP)-coated QCM

Before used, the QCM chip were immersed in piranha solution (H_2O_2/H_2SO_4 = 1/3) for 5 min, then rinsed exhaustively with deionized water and drying with N_2. A solution of peptide (0.1 mg/mL) and dopamine was mixed thoroughly in Tris–HCl buffer (20 mM, pH = 8.5). After depositing 200 μL of the aliquot on QCM chip, the chip was placed horizontally for 6 h at room temperature. Then the polydopamine coated QCM chip was washed with water containing 5% acetic acid for five times, followed by a wash with deionized water to remove the template and drying.

The non-imprinted polymer (NIP) film was prepared as the same procedure of MIP except that in the presence of template.

2.4. Quartz crystal microbalance adsorption measurement

All adsorption experiments were performed by using QCM (KSV model QCM-Z500) at 26 °C. For each measurement, Tris–HCl buffer (20 mM, pH = 7.0) was first injected into the sample cell to obtain a stable baseline (about 10 min to reach equilibrium). Then, the template peptide or protein with different concentration was injected into the sample cell. The frequency of the QCM sensor decreased rapidly and reached a steady value within 10 min. The adsorbed mass, Δm (g) on QCM chips after equilibrium is registered as changes in frequency, Δf (Hz) through the Sauerbrey equation (Eq. (1)) (Ouyang et al., 2007):

$$\Delta m = -\frac{C}{n}\Delta f \quad (1)$$

where C is the mass sensitivity constant and n denotes the number of overtone (n = 1, 3, 5, ...). In this paper, only the normalized frequency shifts of fifth harmonic was represented.

3. Results and discussion

3.1. Formation of MIP coatings on QCM

The fusion protein (glycoprotein gp41) of human immunodeficiency virus type 1 (HIV-1 gp41) is an expensive biomacromolecule, which is not suitable as template for molecular imprinting. In this paper, the synthetic peptide of gp41 fragment 579–613 was used as template to prepare a quartz crystal microbalance (QCM) biomimetic sensor. Dopamine was used as functional monomer and crosslinking agent. During polymerization of dopamine, the synthetic peptide was embedded in the polydopamine film through the molecular recognition events (maybe including hydrogen bond, ionic bond and hydrophobic interaction between peptide and dopamine). Removal of the template left behind imprinted recognition sites which are complimentary to the template in terms of shape, size, and distribution of functional groups (Fig. 1).

The formation of polydopamine film was first monitored by X-ray photoelectron spectroscopic (XPS) measurements (Fig. 2). In XPS spectrum, the peaks of C1s at 284.75 eV, N1s at 399.9 eV and O1s at 532.4 eV in the survey spectrum was clearly observed (Fig. 2A). The ratio of nitrogen to carbon (N/C) peak areas was 0.119, which was near to the theoretical value of 0.125 of dopamine (Lee et al., 2007), indicating the polymer was formed from the polymerization of dopamine. The fitted C1 s XPS spectrum (Fig. 2B) displays three peaks at 284.45 eV, 286.02 eV and 287.95 eV attributed to C–C, C–N and C–O groups, respectively, which are in good accordance with the assumed chemical composition of the polymer film (Ouyang et al., 2007).

Then the FT-IR spectrum was used to further verify the composition of polymer (Supporting material, Fig. S1). The peaks at 1280 cm^{-1} and 1341 cm^{-1} may be assigned to bending vibrations of O–H and stretching vibration of C–OH. The spectrum also showed two typical absorption peaks of phenyl group at 1512 cm^{-1} and 1600 cm^{-1} (Ouyang et al., 2010). The broad band between about 3200 cm^{-1} and 3400 cm^{-1} may be contributed to the stretching vibration of free –OH or $–NH_2$, which is in the accordance with the composition of dopamine. All these groups provide an evidence for multifunctional binding sites to the template molecules.

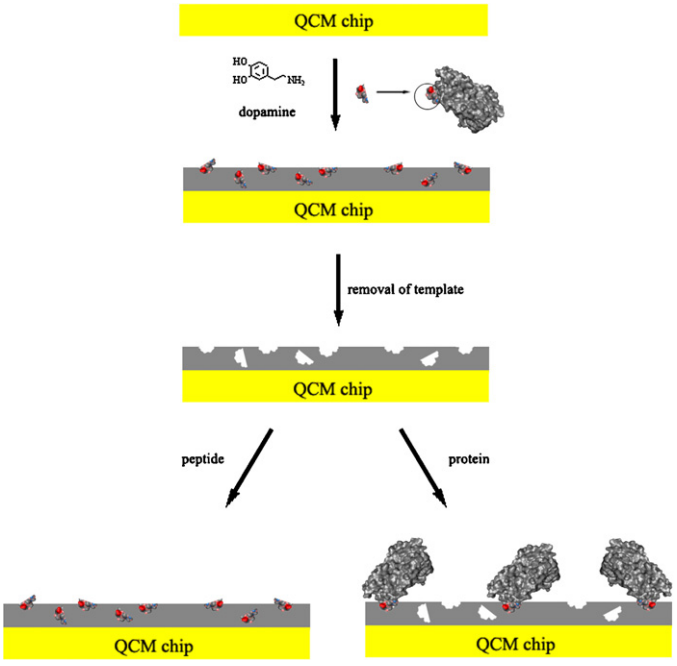

Fig. 1. Schematic diagram representation of epitope-imprinting.

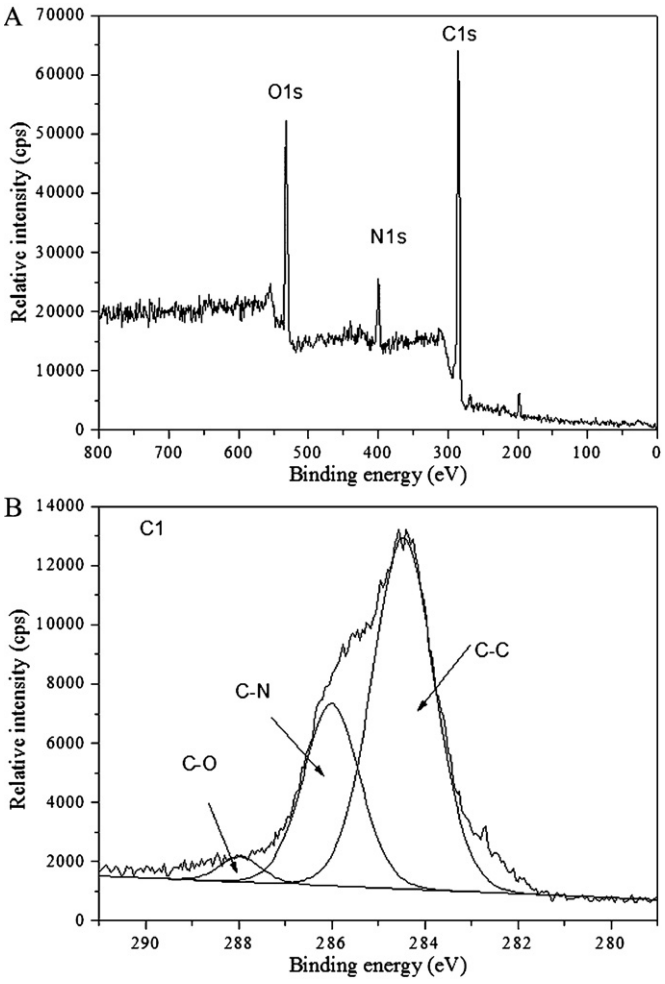

Fig. 2. XPS survey (A) and fitted C1s (B) spectra of polydopamine prepared without template.

3.2. Characterization of surface morphology

The surface morphology of the obtained QCM chip was characterized by AFM. Each scan represents a 1.0 μm × 1.0 μm lateral area and the vertical scale is 20 nm per division. From the AFM images (Supporting material, Fig. S2), the root mean-square (RMS) roughness of MIP and NIP was obtained to be 1.95 and 1.77, respectively, which were both higher than that of bare QCM chip, indicating that the polydopamine films were successfully synthesized on QCM chip. Meanwhile, the similar RMS value of MIP and NIP film indicated that there are no apparent morphological differences between MIP and NIP films.

3.3. Effect of dopamine concentration

In the process of peptide imprinting, dopamine was polymerized to form thin film on the surface of QCM chip. The thinness of polydopamine film would have a great effect on the distribution of recognition sites, which affect the rebinding capability of MIP film to the template directly. Thus, the film thickness which was controlled by the concentrations of dopamine is important in this work. Fig. S3 (Supporting material) illustrates the effect of dopamine concentrations on the rebinding capability. It is clearly that when 50 ng/mL of the template was injected, the MIP-coated QCM chip reached a maximum binding amount at 5 mg/mL of dopamine. This may be due to the fact that when less dopamine was used, the thin polymer film was distributed unevenly on the surface of QCM chip,

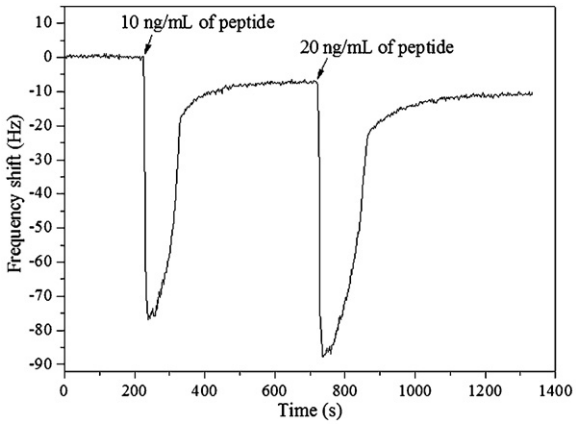

Fig. 3. Changes in MIP-coated QCM frequency in response to different concentrations of template (10 ng/mL and 20 ng/mL of peptide). After the addition of template, the frequency of the sensor decreased rapidly and reached a steady value within 10 min.

thus the low density of the recognition sites would result in less rebinding of the template. On the contrary, when the concentration of dopamine larger than 5 mg/mL, thick polymer film was form on the surface of QCM chip. Because the template concentration was fixed at 50 ng/mL, the thicker film would decrease the density of recognition sites and lead to the decrease in rebinding. Therefore, 5 mg/mL of dopamine was chosen in this study.

3.4. Imprinting effect

Fig. 3 showed the frequency–time response of MIP-coated QCM chip towards the template peptide at a concentration of 10 ng/mL and 20 ng/mL. It is clearly that when the analyte was injected, frequency of the MIP-coated QCM sensor decreased rapidly and reached a steady value within 10 min. This result suggested that the binding of template molecules to the MIP film was a fast process.

The MIP/NIP-coated QCM chips were tested on-line at 26 °C to investigate the affinity of imprinted film to the template in the concentrations range from 2 ng/mL to 200 ng/mL. Fig. 4A showed the adsorption isotherms of template peptide bound to the imprinted film and non-imprinted film. As shown in the Fig. 4A, the changes in frequency of QCM, Δf (Hz) increased as increasing of the template concentrations and reach equilibrium at 100 ng/mL, which demonstrated the increasing adsorption of the template molecule on the QCM chip below 100 ng/mL. Meanwhile, the MIP-coated QCM chip exhibited a higher frequency change for template than that of NIP-coated QCM chip at the same concentration. For example, the maximal frequency shifts of the MIP-coated QCM sensor towards the template was 15.13 Hz, whereas the NIP-coated sensor responded only 1.799 Hz at maximum. This result clearly indicated that the imprinted cavities fit the size and shape of the template molecule used for imprinting and the resulting MIP-coated QCM chip has specific affinity for the template peptide. The low adsorption of peptide to the non-imprinted film may be attributed to nonspecific binding.

To further investigate the binding behaviors of MIP-coated QCM chip towards the template, the QCM measured data were plotted with Scatchard plot equation (Eq. (2)) (Tai et al., 2005, 2010):

$$\frac{B}{C} = -\frac{1}{K_d}B + \frac{B_{max}}{K_d}B = \frac{\Delta f}{M_w} \quad (2)$$

where C and M_w are the concentration and molecular weight of the analyte, respectively, B is the fraction of sites bound, and K_d is the dissociation constant. We define that $y = B/C$, and $x = B$. Therefore, the Scatchard plot equation was calculated to be

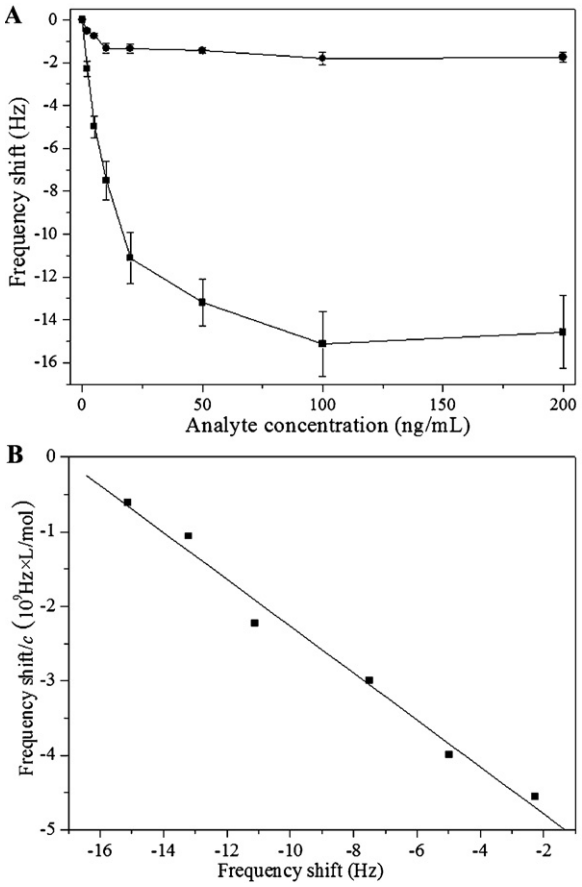

Fig. 4. (A) The corresponding frequency shifts of the MIP-coated electrode (■) and NIP-coated electrode (●) for the different concentrations of HIV-1 gp41 related peptide. The frequency shifts were recorded after the sensor reach equilibrium state. Error bars indicate the standard deviation in triplicated experiments. (B) Scatchard analysis of the binding of template to the MIP film.

$y = -3.1496 \times 10^8 x - 5.4163 \times 10^9$, $R^2 = 0.9851$ (Fig. 4B). From the slope of equation, the K_d value for the template peptide on MIP-coated QCM chip surface was calculated to be 3.17 nM, which is close to some monoclonal antibodies (Alam et al., 2008; Hinz et al., 2009). The small K_d value suggested a high affinity of the MIP to template molecules.

3.5. Selectivity of QCM sensor

Selectivity is a key parameter in preparing molecularly imprinted polymer. In this work, some of other biomolecules (BSA, mutated peptides and the control peptide) were used to further investigate the selectivity of the imprinted film. The data are shown in Fig. 5A. It is clearly that the response of the MIP-coated QCM chip to template peptide was observed almost 6 times higher than that of control peptide and BSA. This result can be traced back to the fact that the recognition sites of MIP film were complimentary to the shape, size and functional-groups of the template, which was preorganized with the functional monomer in imprinting process. In fact, the size of BSA is larger than template peptide and had incorrect spatial orientation of the recognition sites, thus was seldom bound to the MIP film. So is the control peptide with different sequence and functional-groups from the template, which prevents the binding of this peptide to the MIP film. As to 2M-peptide, since it only has two mutated amino acids to the template peptide and has the similar functional-groups to the template peptide, the respond of the MIP-coated QCM chip to 2M-peptide was similar to template peptide. The 11M-peptide

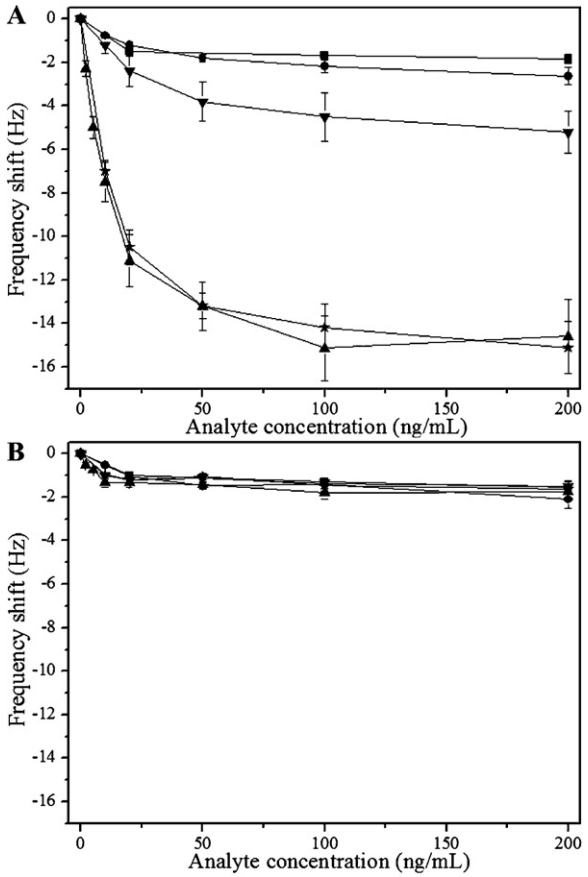

Fig. 5. Responds of the obtained MIP-coated QCM chip (A) and NIP-coated QCM chip (B) to BSA (■), GA-16-NH2 (●), 11M-peptide (▼), 2M-peptide (★) and HIV-1 gp41 related peptide (▲). The frequency shifts were recorded after the sensor reach equilibrium state. Error bars indicate the standard deviation in triplicated experiments.

has eleven mutated amino acids to the template peptide, thus the respond of the MIP-coated QCM chip to 11M-peptide was much lower than template peptide. As to NIP-coated QCM chip, it has a low adsorption of template peptide and other biomolecules due to the nonspecific binding (Fig. 5B). These results can prove that the proposed epitope-imprinting technique is the sequence selective method. The significantly high selectivity of MIP film for the template peptide with respect to other biomolecules further confirmed the success of the imprinting approach.

3.6. Detection of HIV-1 gp41

Based on principle of epitope imprinting, the resultant MIP could recognize not only the template but also the whole macromolecule. In this study, the recognition of MIP-QCM towards the corresponding HIV-1 gp41 protein was also characterized. As shown in Fig. 6, the binding curve for frequency shift against HIV-1 gp41 protein concentration was linear in the range from 5 ng/mL to 200 ng/mL (relative standard deviation (RSD) range from 6.7% to 15.4%, $n = 3$) with the linear equation of $y = -5.8132x + 0.4031$, $R^2 = 0.9928$. The detection limit of HIV-1 gp41 protein was 2 ng/mL, which was comparable to the reported ELISA method. Therefore, this result present that detection of HIV-1 gp41 protein by using MIP-QCM was feasible.

3.7. Detection of HIV-1 gp41 in human urine sample

At last, the obtained MIP-coated QCM sensor was used for selective detection of HIV-1 gp41 in human urine samples. 10 mL of human urine was centrifuged at 3000 rpm for 5 min, followed by diluted with 20 mL Tris–HCl (20 mM, pH = 7.0) before used. Then different concentrations of the HIV-1 gp41 were spiked in the human urine samples mentioned above and determined by MIP-coated QCM sensor. The recovery was in the range of 86.5–94.1% (Supporting material, Table S1). The results suggested the feasibility of this approach to be applied in real samples detection.

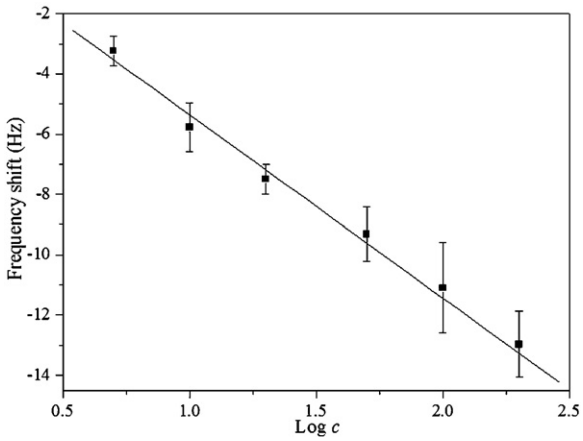

Fig. 6. The corresponding frequency shifts of the MIP-coated electrode for the different concentrations of HIV-1 gp41 protein. The frequency shifts were recorded after the sensor reach equilibrium state. Error bars indicate the standard deviation in triplicated experiments.

4. Conclusions

In this study, we have successfully fabricated a MIP-coated QCM biomimetic sensor for HIV-1 related peptide and protein based on epitope-imprinting techniques, and demonstrated its application for detection of real samples in a real-time manner. High affinity of the peptide-imprinted film towards the template molecule was observed at nanogram range, and the K_d value for the template was circulated to be 3.17 nM. QCM measurement showed that the resulting MIP film not only had a great affinity towards the template peptide, but also could bind the corresponding gp41 protein specifically. Therefore, the obtained MIP-coated QCM sensor was applied successfully for monitoring of HIV-1 gp41 in human urine samples. These results show certain advantages of epitope-imprinting such as high sensitivity and high selectivity for the template molecule and its mother protein. Furthermore, using dopamine as functional monomer made the sensor superior to other MIP sensors, such as high hydrophilicity and biocompatibility. The simplicity of the presented method would put forward the using of epitope imprinting polymers for biomolecules analysis.

Acknowledgments

This work was supported by the National Basic Research Program of China (No. 2010CB732403), the grants from the National Natural Science Foundation of China (No. 20975023), the program for new century excellent talents in university of China (09-0014) and the National Science Foundation of Fujian Province (2010J06003).

Appendix A. Supplementary data

Supplementary data associated with this article can be found, in the online version, at doi:10.1016/j.bios.2011.11.008.

References

Alam, S.M., Scearce, R.M., Parks, R.J., Plonk, K., Plonk, S.G., Sutherland, L.L., Gorny, M.K., Pazner, S.Z., VanLeeuwen, S., 2008. J. Virol. 82, 115–125.
Alexander, C., Andersson, H.S., Andersson, L.I., Ansell, R.J., Kirsch, N., Nicholls, I.A., O'Mahony, J., Whitcombe, M.J., 2006. J. Mol. Recognit. 19, 106–180.
Bossi, A., Bonini, F., Turner, A.P.F., Piletsky, S.A., 2007. Biosens. Bioelectron. 22, 1131–1137.
Bossi, A., Piletsky, S.A., Piletska, E.V., Righetti, P.G., Turner, A.P.F., 2001. Anal. Chem. 73, 5281–5286.
Bui, B.T.S., Merlier, F., Haupt, K., 2010. Anal. Chem. 82, 4420–4427.
Burzio, L.A., Waite, J.H., 2000. Biochemistry 39, 11147–11153.
Burton, D.R., Desrosiers, R.C., Doms, R.W., Koff, W.C., Kwong, P.D., Moore, J.P., Nabel, G.J., Sodroski, Wilson, I.A., Wyatt, R.T., 2004. Nat. Immunol. 5, 233–236.
Buzón, V., Cladera, J., 2006. Biochemistry 45, 15768–15775.
Cai, D., Ren, L., Zhao, H., Xu, C., Zhang, L., Yu, Y., Wang, H., Lan, Y., Roberts, M.F., Chuang, J.H., Naughton, M.J., Ren, Z., Chiles, T.C., 2010. Nat. Nanotechnol. 5, 597–601.
Chan, D.C., Chutkowski, C.T., Kim, P.S., 1998. Proc. Natl. Acad. Sci. U.S.A. 95, 15613–15617.
Contreras, L.M., Aranda, F.J., Gavilanes, F., Gonzalez-Ros, J.M., Villalain, J., 2001. Biochemistry 40, 3196–3207.
Cutivet, A., Schembri, C., Kovensky, J., Haupt, K., 2009. J. Am. Chem. 131, 14699–14702.
Dwyer, J.J., Hasan, A., Wilson, K.L., White, J.M., Matthews, T.J., Delmedico, M.K., 2003. Biochemistry 42, 4945–4953.
Gao, D.M., Zhang, Z.P., Wu, M.H., Xie, C.G., Guan, G.J., Wang, D.P., 2007. J. Am. Chem. 129, 7859–7866.
Ge, Y., Turner, A.P.F., 2008. Trends Biotechnol. 26, 218–224.
Ge, Y., Turner, A.P.F., 2009. Chem. Eur. J. 15, 8100–8107.
Haupt, K., 2003. Anal. Chem. 75, 376A–383A.
He, H., Fu, G., Wang, Y., Chai, Z., Jiang, Y., Chen, Z., 2010. Biosens. Bioelectron. 26, 760–765.
Hinz, A., Schoehn, G., Quendler, H., Hulsik, D.L., Stiegler, G., Katinger, H., Seaman, M.S., Montefiori, D., Weissenhorn, W., 2009. Virology 390, 221–227.
Hoshino, Y., Kodama, T., Okahata, Y., Shea, K.J., 2008. J. Am. Chem. 130, 15242–15243.
Lee, H., Dellatore, S.M., Miller, W.M., Messersmith, P.B., 2007. Science 318, 426–430.
Li, J., Jiang, F., Li, Y., Chen, Z., 2011. Biosens. Bioelectron. 26, 2097–2101.
Li, Y., Yang, H.H., You, Q.H., Zhuang, Z.X., Wang, X.R., 2006. Anal. Chem. 78, 317–320.
Nematollahzadeh, A., Sun, W., Aureliano, C.S.A., Lütkemeyer, D., Stute, J., Abdekhodaie, M.J., Shojaei, A., Sellergren, B., 2011. Angew. Chem. Int. Ed. 50, 495–498.
Nishino, H., Huang, C.S., Shea, K.J., 2006. Angew. Chem. Int. Ed. 45, 2392–2396.
Ouyang, R.Z., Lei, J.P., Ju, H.X., 2007. Adv. Funct. Mater. 17, 3223–3230.
Ouyang, R.Z., Lei., J.P., Ju., H.X., 2008. Chem. Commun. 44, 5761–5763.
Ouyang, R.Z., Lei, J.P., Ju, H.X., 2010. Nanotechnology 21, 185502–185511.
Pernites, R., Ponnapati, R., Felipe, M.J., Advincula, R., 2011. Biosens. Bioelectron. 26, 2766–2771.
Polyakov, M.V., 1931. Zh. Fiz. Khim. 2, 799–805.
Rachkov, A., Minour, N., 2000. J. Chromatogr. A 889, 111–118.
Riskin, M., Tel-Vered, R., Bourenko, T., Granot, E., Willner, I., 2008. J. Am. Chem. 130, 9726–9733.
Riskin, M., Tel-Vered, R., Lioubashevski, O., Willner, I., 2009. J. Am. Chem. 131, 7368–7378.
Shi, H.Q., Tsai, W.B., Garrison, M.D., Ferrari, S., Ratner, B.D., 1999. Nature 398, 593–597.
Stringer, R.C., Gangopadhyay, S., Grant, S.A., 2010. Anal. Chem. 82, 4015–4019.
Tai, D.F., Jhang, M.H., Chen, G.Y., Wang, S.C., Lu, K.H., Lee, Y.D., 2010. Anal. Chem. 82, 2290–2293.
Tai, D.F., Lin, C.Y., Wu, T.Z., Chen, L.K., 2005. Anal. Chem. 77, 5140–5143.
Tan, J., Wang, H.F., Yan, X.P., 2009. Anal. Chem. 81, 5273–5280.
Tatemichi, M., Sakamoto, M., Mizuhata, M., Deki, S., Takeuchi, T., 2007. J. Am. Chem. 129, 10906–10910.
van der Leeden, M.C., 2005. Langmuir 21, 11373–11379.
Vlatakis, G., Andersson, L.I., Müller, R., Mosbach, K., 1993. Nature 361, 645–647.
Wang, H.J., Zhou, W.H., Yin, X.F., Zhuang, Z.X., Yang, H.H., Wang, X.R., 2006. J. Am. Chem. 128, 15954–15955.
Wulff, G., 1995. Angew. Chem. Int. Ed. 34, 1812–1832.
Wulff, G., Sarhan, A., 1972. Angew. Chem. Int. Ed. 11, 341–344.
Ye, L., Mosbach, K., 2008. Chem. Mater. 20, 859–868.
Zhang, W., He, X.W., Chen, Y., Li, W.Y., Zhang, Y.K., 2011. Biosens. Bioelectron. 26, 2553–2558.
Zeng, Z., Hoshino, Y., Rodriguez, A., Yoo, H., Shea, K.J., 2010. ACS Nano 4, 199–204.
Zhou, W.H., Lu, C.H., Guo, X.C., Chen, F.R., Yang, H.H., Wang, X.R., 2010. J. Mater. Chem. 20, 880–883.